# Virtual Torque Based Control of Three Phase Rectifier Under Grid Imbalance and Harmonics

Grzegorz Iwanski, *Member, IEEE*, Tomasz Luszczyk, and Mateusz Szypulski, *Student Member, IEEE*

***Abstract*—The paper deals with a new control method of three phase rectifier operating under simultaneous grid voltage imbalance and harmonics. The proposed method uses virtual electromagnetic torque, which is calculated on basis of converter current and virtual flux of the power grid. Direct calculation of reference alpha/beta components of current vector does not require any synchronization procedure or grid voltage/virtual flux orientation of the reference frame. On the other hand, the proposed control is still as simple in implementation as other vector control methods, such as voltage oriented control or virtual flux oriented control. The introduced variable (virtual torque) allows to calculate reference current vector components in alpha/beta frame without symmetrical components decomposition. The current vector obtained using the proposed control method has the same asymmetry factor as unbalanced grid voltage. It means that the rectifier is seen by the grid as a resistive load with the same resistance in each phase. For the grid it is preferable target, because the phase with the highest voltage is loaded most, while the other phases are less loaded. Converter power can be increased by progressive balancing of three phase converter current keeping the phase current limit.**

***Index Terms*—AC-DC power conversion, current control, current limiters, torque control.**

## I. Introduction

UNBALANCED grid operation of power converters (Fig. 1) is currently strongly investigated in publications on power electronic grid interfaces. Simultaneously, the grid harmonics have strong influence on power quality of grid converters and the problem becomes significant due to increasing amount of higher harmonics consumed by nonlinear loads. Initially, grid imbalance and harmonics have not been taken into consideration in grid converter control methods. Firstly, there were used hysteresis controllers of converter current [1][2] or instantaneous power components (DPC) [3][4] due to simple implementation in analog technology. Later, converter current control (vector control) [5][6] or instantaneous power components control (DPC-SVM) with digitally implemented linear regulators were used. The orientation of reference frame along grid voltage vector makes a problem of determination of reference frame rotation angle. Grid voltage harmonics produce transformation angle oscillations, which implicate converter current distortions.

The Work is supported by National Science Centre within the Project granted on the basis of the decision number DEC-2011/01/B/ST7/05836 and within the statutory funds of Warsaw University of Technology

Authors are with the Institute of Control and Industrial Electronics, Warsaw University of Technology, 00-662 Warszawa, Poland (corresponding author contact phone: +4822 2347415; fax: +4822 2346023; e-mail: iwanskig@isep.pw.edu.pl)

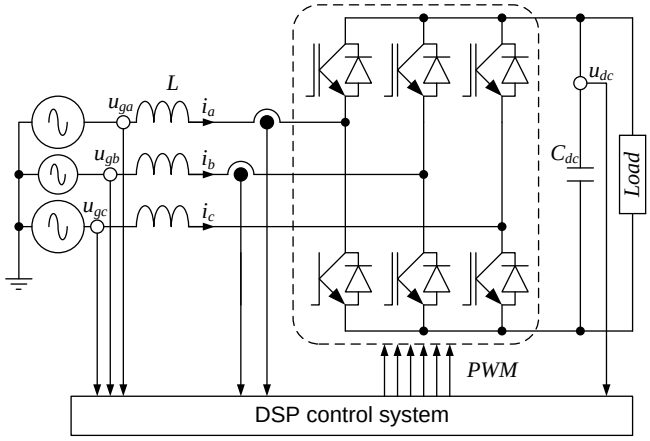


Fig. 1. Scheme of the analyzed three-phase three-wire active rectifier connected to unbalanced grid.

In order to obtain sinusoidal balanced current under grid voltage harmonics, some improvements have been proposed, mainly phase locked loops PLL, or virtual flux orientation [7][8] to find the phase angle of fundamental frequency component. Seeing that the PLL can be used to find the position of positive sequence vector component, content of the positive and negative sequences in virtual flux is the same as in the grid voltage, based on which the virtual flux is calculated. Thus, the angle of virtual flux vector cannot be used directly as the *dq* reference frame rotation angle, without prior determination of positive sequence component of virtual flux vector. Modifications of the classic current and power control methods dedicated to operation with unbalanced grid assume usually symmetrical converter current target. This target can be reached without the sequence decomposition, but in many papers it has been proposed [9]-[11] as the first solution. Symmetrical currents can be obtained by fixing *d* and *q* components of reference current vector and simultaneously using proportional-integral-resonant controllers in reference frame oriented with the positive sequence of voltage (or virtual flux) vector. Current limitation can be obtained by limitation of the vector length, which is fixed independently of the voltage asymmetry in this target. In [12][14] it has been proposed to impose unity power factor in each phase with simultaneous current imbalance corresponded to the grid voltage imbalance. In this case, methods of converter phase current limitation that have been developed are based on the separate determination of reference converter current symmetrical components [15][16].

There are proposed in the literature other strategies for rectifiers operating with unbalanced grid. One of them is to keep constant *p* component of power to remove DC voltage

oscillations. In order to reach sinusoidal converter current an adequate *q* power component oscillations have be determined and referenced. However, this method makes the current hodograph 90 degrees rotated in relation to the grid voltage hodograph. It means that a phase with lowest voltage is loaded most, and from the grid point of view it is unwanted rectifier target. The other strategy, which is considered in publications, is to obtain current imbalance corresponding to the grid voltage imbalance [14]-[20]. This target does not deepen the voltage asymmetry, because the phase with higher voltage is more loaded than others. However, in such a case the problem of current limitation have to be solved in another way, because current vector length is no longer fixed.

In [21] the virtual flux vector components are assigned in a standard way by voltage integration, but later the equations for power components determination (numbered (4)(5) in the cited paper), based on the flux vector components are taken from [7]. These equations are valid only for symmetrical sinusoidal voltage. It is assumed that $\alpha\beta$ components of virtual flux vector are the $\beta\alpha$ components of voltage vector scaled by grid voltage pulsation. It is not true for asymmetrical voltage, because $\alpha\beta$ components of voltage vector have different amplitudes or/and different than $\pi/2$ phase shift. The method of reference frame orientation can be used for the voltage distorted by harmonics (it has been proved in [7]), but not for the asymmetry. Finally, in the paper, to achieve satisfactory results, there is used PLL structure to assign orientation of positive sequence component of virtual flux. However in this frame, the power calculated by presented equations does not represent the Akagi's power, but another variable which is constant for symmetrical virtual flux and for symmetrical current, which is a wanted target in this paper. The cited paper is an example that the classic virtual flux method without PLL does not provide satisfactory results. On the other hand, when PLL structure is applied, it can be obtained the same on the basis of the voltage vector without using virtual flux calculation.

In [22] the Authors want to achieve unity power factor in each phase through elimination of instantaneous power *p* component oscillations (constant *p* component of power defined by Akagi), but at the same time they want zero phase shift between converter current and grid voltage in each phase. This cannot be achieved simultaneously, because zero phase shift between current and voltage can be achieved only for pure resistive load (it means active rectifier is seen by the grid as a resistor) and only for this case, the condition is met. Then, the *q* component of instantaneous power is zero, but the *p* component responsible for energy transfer oscillates due to the voltage and current imbalance. Constant *p* and oscillating *q* component of power causes opposite orientation of unbalanced current vector hodograph to the unbalanced grid voltage vector hodograph, but in this case there is a phase shift between current and voltage in at least two phases. It cannot be obtained with a resistive load. Obtained phase shift between current and voltage in each phase is close to zero, what results from the relatively low voltage asymmetry and the measurement of voltage in relation to the source neutral point, instead of virtual neutral point. In such a case the measured voltage contains zero sequence and indicated phase shift between current and voltage is lower than it is in relation to the voltage seen by the converter (without zero sequence component).. It has to be noted that presented target, which is constant *p* component of instantaneous power and sinusoidal (although unbalanced) converter current, is achieved. The only inconsistency is that Authors treat this target as operation with unity power factor and zero phase shift between current and voltage, what is not true. However, for the presented indirect matrix converter the character of the load side *p* component of instantaneous power and grid side *p* component of instantaneous power will be the same.. Thus, other target than presented in the paper cannot be achieved in the proposed topology for symmetrical load and constant output (load side) *p* component of power. Additionally any *p* power oscillations produced during nonlinear load supply will be transferred to the grid independently of grid voltage symmetry or asymmetry. This is one of drawbacks of all power converter topologies without intermediate DC bus.

Constant *p* component of instantaneous power at grid voltage imbalance has been proposed for Vienna Rectifier for elimination of oscillations of DC voltage used directly for load supply [23]. This target is beneficial for the load sensitive on the voltage variations, but it is not beneficial for the grid at rectifier mode operation of the grid converter. In opposition to the cited paper, in the following paper it is proposed orientation of the current vector hodograph corresponding to the orientation to the voltage vector hodograph as the basic target for rectifier mode operation, which is beneficial for the grid, whereas not all types of load supplied from active rectifier are sensitive to the DC voltage oscillations. In the cited paper, the Authors do not propose the current balancing in the case, in which lack of energy occurs in DC link, but they set the current limit at the level giving the maximum length of the current vector equals to the maximum length of vector for circular hodograph representing symmetrical current. In the case of unbalanced current it does not provide true limitation of phase current as well as maximum power transfer.

The papers [24] and [25] are about similar control strategy of constant *p* and *q* components of instantaneous power, wherein the *q* component of power is calculated according to modified instantaneous power theory by Kawabata, that means as the dot product with the use of unbalanced grid voltage vector $\alpha\beta$ components shifted by 90 degrees. The *q* component calculated this way is constant only for this target (opposite hodograph of unbalanced current vector in relation to the unbalanced voltage vector). In rectifier it is unwanted target for the grid, because the phase with lower voltage is loaded more, whereas rectifier mode is described in both cited papers. In the paper with switching table, one of the simulation results shows oscillograms with unbalanced voltage and simultaneous harmonics content. Applied harmonics in the grid voltage have significant influence on the actual power components, what needs the current harmonics for compensation of power oscillations caused by grid voltage harmonics. In the following paper to avoid current harmonics in the case of distorted grid voltage, it is proposed a band-pass filtration of measured grid voltage before calculation of reference current signals. In both papers, there are not presented DC link voltage waveforms or transient states.

Arbitrarily referenced step of *p* power component suggests, in opposition to presented schemes, that there was not applied DC link voltage controller in outer loop in both simulation and experimental tests.. However, for the proposed target, the proposed DC link voltage regulation structure may work, because constant *p* does not produce DC link voltage oscillations, but for other targets with oscillating *p* power, the DC link voltage oscillates. Thus, it requires filtration of measured DC voltage signal by additional band-stop filters for 100Hz and optionally for higher frequencies. In both papers [24][25], the current limitation problem is not taken into consideration, and regulation without intermediate current calculation is difficult in realization for power components.

In [26] Authors propose independent controllers for positive and negative sequence components in a respective coordinate frames with the use of PI regulators. There is analyzed only basic target which is symmetrical current, for which the current limitation is quite trivial, because it concerns only the issue of current vector length limitation for circular hodograph. Authors analyze only one target with elimination of negative sequence component or negative and zero sequence in some specific case. The used control is known from earlier publications and called a double synchronous reference frame control. The use of PI controllers for 50Hz zero sequence compensation does not always provide expected results. The current components controlled in *dq* frame are poorly stabilized when zero sequence component occurs, what can be observed in Fig. 9 in the cited paper. In the transient state a significant over-current is observed at initial state. There is some inconsistency, because the current oscillations do not produce power oscillations. Equations numbered (16a)(16b) in the cited paper, presents average values *P1* and *Q1* and not *P* and *Q* respectively. Even for lack of negative and zero sequence components of controlled current, there are not taken into consideration instantaneous power oscillations caused by negative sequence voltage and positive sequence current, while the symmetrical current and unbalanced voltage produce the *p* and *q* power oscillations.

All main possible targets for grid converter, that means current asymmetry opposite to the voltage asymmetry, current asymmetry in accordance to the voltage asymmetry, and symmetrical current, have been analyzed in [27]. Due to the control of power components with additional compensation terms there are not applied current limitations. Authors show the possibility of selected compensation of power or current oscillations, but the selected target is chosen arbitrarily without any superior criteria for the target change. Some algorithms for control parameters selection in each individual target have been proposed, but the targets are selected arbitrarily and they are treated as separate issues. The paper is focused on the inverter operation, and the DC link is supplied from battery, so the DC link voltage controller has not been applied. However even for such a case, the transients caused by step change of reference *p* or *q* component of instantaneous power should be presented to evaluate the control method properties.

Constant *p* power component and sinusoidal unbalanced current target is justified and beneficial for inverter mode operations in the power generating systems, because the phase with lower voltage is supported by higher current [28]. However, analysis of current limitation is not completely correct, because limitation of the maximal vector length to the value of radius of maximum current circular hodograph does not provide true phase current limitation at current imbalance in all cases. It is confirmed by the Figure 14a from the cited paper which shows simulation results, that during asymmetrical voltage sag, the current in every phase does not reach the limit, reached before the sag, whereas the case is described as current limitation. Current waveforms, as well as the step response on reference signals or load change have not been shown in the experimental tests.

The paper [29] describes operations of four-leg converter able to control zero sequence component in the four-wire grid for energy generation. However, assuming elimination of zero sequence current in four-wire system, even in the case of zero sequence voltage presence, casts doubt on the sense of using four-wire system for power converter based energy source. The same can be naturally achieved in the three-wire system topology, where the zero sequence cannot flow without additional control structures dedicated to zero sequence management. Although the targets related to the content of positive and negative sequence have been achieved, the current contains huge amount of higher harmonics. The interesting point of the paper is introduction of a factor allowing flexible targets change and reaching intermediary states. However, the DC voltage oscillations not necessarily should be the main criteria of the factor assignment in most cases, but the phase currents values and operation mode (inverter or rectifier) should be. The issue of current limitation has not been analyzed in the paper [29].

Reference vector components, independently of positive and negative sequence current, but depending on the required target (constant *p* component, constant *q* component, symmetrical current), have been introduced in [30]. Authors refer to the earlier publications in which only *p* component oscillations cancellation target was described and they proposed other targets described as new. However, described the other targets had been known in previous publications, and the Authors were not first. Presented experimental results for all targets are unsatisfactory from the point of view of current harmonics content. High harmonics occur even for symmetrical grid voltage, what means, that there is some fundamental error in either the equations or their implementation. It is difficult to find this error out, because only reference signal calculation has been described thoroughly, whereas the used method of signals decomposition and used internal control structure of positive and negative sequence current are neglected in the description. The experiment made on the power converter with 24V in the DC link and 4.9mH of filter inductance should provide the results which do not rise significant doubts. Due to the use of battery in the DC link, there is lack of DC voltage controller and its operation during transients like step response on the reference power change in the inverter mode, or step response on the load change in the rectifier mode. The used 27mH filter inductor for 300kW simulated inverter is unacceptable in practice.

In the case of independent control of positive and negative sequence components of converter current, the obtained

current quality depends not only on correct reference signals assignment, but on the current control structure, and on the decomposition of measured current into positive and negative sequences as well as the filters used for this purpose. In [31] there is shown an example of independent reference and control of current positive and negative sequences. The paper is about current control and shows the results of arbitrarily referenced positive and negative sequences of converter current without any superior power management and without DC voltage controller. Authors propose some modifications of double synchronous reference frame DSRF control by introduction of some decoupling structure between positive and negative sequence to reduce the mutual influence between the symmetrical components. Authors compare their proposal with a very basic structure known from previous publications, but since the time of publishing this old structure, there have been proposed lots of modifications, which have not been compared and discussed in the paper. Finally, the quality of current obtained by modified DSRF is average and better results were obtained in the papers describing other modifications of DSRF control of converter current.

## II. Converter Current Limitation at Grid Voltage Asymmetry

### A. Limitation of balanced sinusoidal converter current

The reference calculation of constant *d* component of current vector can be made by PI controller of DC link voltage. It is required simultaneous filtration of 100Hz and 300Hz oscillations of actual DC link voltage oscillations caused by negative sequence and dominating ($5^{th}$ and $7^{th}$) grid voltage high harmonics. In case of high amount of harmonics other than $5^{th}$ and $7^{th}$, it can be used low-pass filter LPF, with e.g. 150Hz of cut-off frequency (Fig. 2), instead of 300Hz band-bass filter. Reference *q* component of current vector (responsible for reactive power) can be set arbitrarily at zero, as it is usually done in active rectifiers. Then, the current limitation is made together with anti-windup of PI controller of DC link voltage. However, there is an option in this control structure to introduce control of average value of *q* instantaneous power component. The controller responsible for *q* power component regulation references $i_q^*$ component of current. Reference vector length limitation is made in polar coordinates. This simple limit is applicable only to the balanced sinusoidal current strategy. When the limited length $|i|^{limit*}$ is higher than originally referenced length $|i|^*$, some normalized factor is introduced to reduce the reference *q* component of current. This way the priority for active power is kept when the reference current vector length is going to exceed the limit. Controllers of DC voltage and *q* component have separate anti-windup structures.

### B. Limitation of sinusoidal unbalanced phase current

Fig. 3 presents two elliptical current hodographs. One (Fig. 3a) represents current asymmetry for the maximum vector length $|i|_{max}$, which does not exceed the radius of circular hodograph representing maximum symmetrical current. In this case the three phase currents $i_a$, $i_b$, $i_c$ are lower than their limits. The second hodograph (Fig. 3b) is created to obtain maximum elliptic area inscribed inside a hexagon.

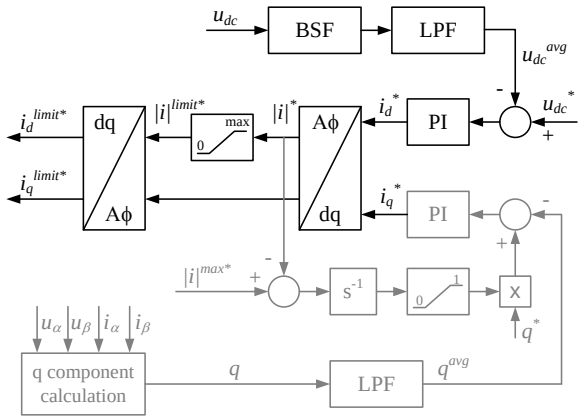


Fig. 2. Control of active rectifier for symmetrical sinusoidal current target with optional non-zero reference reactive power (average value of *q*).

The maximum amplitude of phase current $i_a$, $i_b$, $i_c$ can be reached at least in one phase [18]. Symmetrical grid converter current allows higher power transferred to the DC link than unbalanced current under the same conditions (the same grid imbalance and phase current limit). This is the reason for changing control targets during rectifier operation under variable load. Smooth changing between hodographs from elliptical to circular seems to be preferable. It means progressive balancing of the currents when at least one of the phase currents reaches the limit. Exemplary hodographs obtained this way for increasing power are shown in Fig. 4.

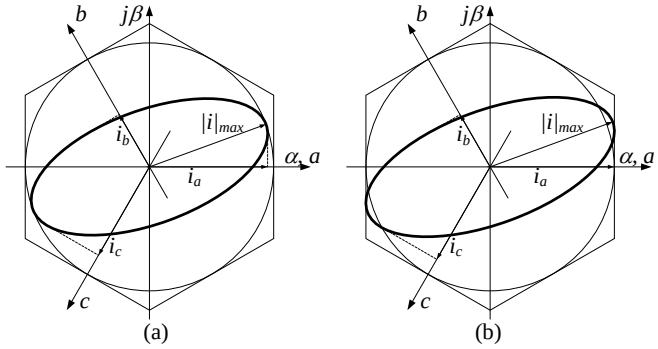


Fig. 3. Possible hodographs of unbalanced current with different ways of applied current limitation giving sinusoidal phase current, a) limitation of the maximum vector length equals to the vector length of maximum symmetrical current, b) true limitation of the phase currents at least in one phase.

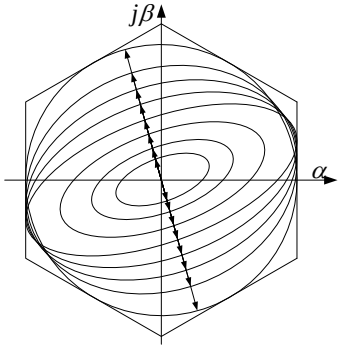


Fig. 4. Possible hodographs of unbalanced current during progressive change.

The target of opposite asymmetry of current in relation to asymmetry of grid voltage is beneficial for the DC voltage oscillations cancellation, because at this target the *p* component of power (defined by Akagi) is fixed, so the energy

transfer from grid to the DC link is constant. However, it is not beneficial for the grid, because the phase with lower voltage is loaded more. This target is recommended for inverter mode of operation, because it can support more the grid in the phase with lower voltage. The maximum amount of transferred power is the same for both targets – current asymmetry accorded to the voltage asymmetry and current asymmetry opposite to the voltage asymmetry, and is lower than for symmetrical current target. Thus, a progressive balancing of current may be applied in case of the energy deficit in the DC link in rectifier mode of operation.

### C. *Limitation of instantaneous value of unbalanced current*

Other methods of current limitation will be compared in this paper in the section with simulation and experimental results to show an advantage of the proposed methods of current limitation and progressive current balancing. The Fig. 5 shows the current hodographs for other methods of current limitation, which do not provide sinusoidal phase currents when the unbalanced sinusoidal current is originally referenced before limitation. Fig. 5a presents the case in which the current vector instantaneous length is cut when it originally exceeds the maximum value, but it is remained unchanged when it is lower than the limit. Finally the hodograph is piecewise circular and piecewise elliptic. This is reached when the adequate for symmetrical current classic current limitation, which is shown in Fig. 2, is applied to the originally referenced unbalanced current. The second method (Fig. 5b) limits the current vector when its length exceeds the hexagon. This is equivalent to the limitation of phase current instantaneous value, without consideration whether its rms value exceeds the limited rms or not. In both cases, if the limitation is not applied, the vector length exceeds both circular hodograph and hexagon, what results in exceeding the limit by both instantaneous and rms value is some phases, despite sinusoidal current in each phase.

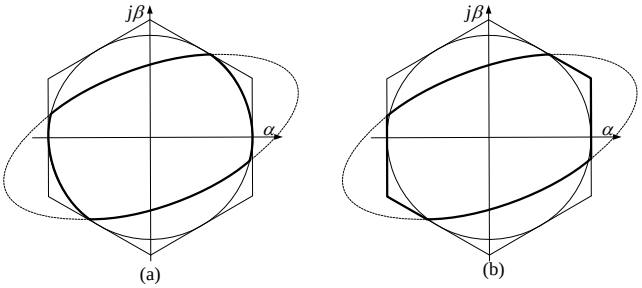


Fig. 5. Possible hodographs of unbalanced current with different ways of current limitation giving non-sinusoidal phase current, a) limitation of the vector length equal to the vector length of maximum symmetrical current, b) limitation of the phase currents instantaneous values.

## III. Calculation of the Reference Current without Sequence Decomposition

### A. *Concept of the virtual torque*

It is known the concept of the power network treated as virtual machine in the virtual flux oriented control method [7][8]. Until now, the concept of virtual machine has been used to change the reference frame orientation from the grid voltage to virtual flux. The virtual flux obtained by integration of grid voltage is less distorted by higher harmonics.

The flux of virtual machine can be calculated typically in the same manner like in variable speed motor control with commonly neglected stator resistance:

$$\psi_g = \int u_g dt \tag{1}$$

In order to eliminate constant component caused by voltage sensors offsets and initial conditions, usually pre-filters are applied. However, due to nearly constant frequency of the grid voltage, therefore also of the virtual flux, the integration action can be replaced by second order low-pass filter with cut-off frequency equals to 50Hz, damping ratio equals 1, and gain $2/\omega_s$, which provides 90 degrees phase shift for this frequency and adequate amplitude of the output signal (virtual flux) at 50Hz. The second order low-pass filter is effective and true for the voltage having the frequency close to the cut off frequency like it is in the grid, and this manner cannot be used in other systems like in variable speed induction motors requiring variable frequency of the supply voltage. Earlier, the grid voltage components in $\alpha\beta$ frame are filtered by 50Hz band-pass filters to remove high harmonics from the measured voltage and for reduction of integration starting point influence. The scheme of proposed virtual flux calculation is presented in Fig. 6. Fundamental harmonic grid voltage and virtual flux components will be further used for calculation of reference current components. The proposed method of virtual flux calculation removes the transient component of flux, but it is virtual flux and not real flux of the machine and for assumed purpose the transient component of flux is not needed.

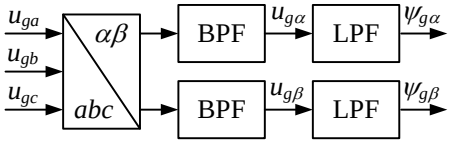


Fig. 6. Method of grid voltage and virtual flux fundamental harmonics determination in $\alpha\beta$ frame.

The concept of virtual machine can be utilized for calculation of its torque, which is constant for the same voltage and current asymmetry factor and the same asymmetry character. Simultaneously, in this case the $q$ component of instantaneous power, calculated according to the standard Akagi's theory, is fixed. This has been found in the doubly fed induction machine operating with unbalanced grid [32], but in a grid converter structure the calculated virtual torque is only an auxiliary variable.

Equations of grid connected active rectifier in $\alpha\beta$ stationary frame are well known (2)(3)

$$u_{c\alpha} = R_L i_\alpha + L\frac{di_\alpha}{dt} + u_{g\alpha} \tag{2}$$

$$u_{c\beta} = R_L i_\beta + L\frac{di_\beta}{dt} + u_{g\beta} \tag{3}$$

in which $u_g$, is the grid voltage vector, $i$ is the current vector, $u_c$ is the voltage vector created by the power converter, $R_L$ is the inductor resistance, and $L$ is the filter inductance.

Additional power balance converted equation is related to the DC link circuit (4)

$$\frac{p}{u_{dc}} - i_{ld} - C_{dc}\frac{du_{dc}}{dt} = 0 \tag{4}$$

where $i_{ld}$ is the load current, and $p$ is the component of power calculated by (5) with neglected losses on the filter resistance.

$$p = \frac{3}{2}\left(u_{g\alpha}i_{\alpha} + u_{g\beta}i_{\beta}\right) \tag{5}$$

The virtual torque can be calculated using (6)

$$T_v = \frac{3}{2}\left(\psi_{g\alpha}i_{\beta} - \psi_{g\beta}i_{\alpha}\right) \tag{6}$$

in which $i_{\alpha}$, $i_{\beta}$ are converter current vector components in $\alpha\beta$ coordinates, $\psi_{g\alpha}, \psi_{g\beta}$ – virtual flux vector components.

### B. *Calculation of the reference current based on reference the virtual torque and q component of instantaneous power*

According to the instantaneous power theory, which is useful for control of power conversion systems, instantaneous power component $q$ can be calculated (7):

$$q = \frac{3}{2}\left(u_{g\beta}i_{\alpha} - u_{g\alpha}i_{\beta}\right) \tag{7}$$

Based on equations (6)(7), and replacement of the actual variables by the reference ones, the current vector components can be derived as the function of reference virtual torque $T_v^*$ and reference $q^*$ component of instantaneous power (8)(9).

$$i_{\alpha}^* = \frac{2}{3}\frac{q^*\psi_{g\alpha} + T_v^*u_{\alpha}}{u_{g\beta}\psi_{g\alpha} - u_{g\alpha}\psi_{g\beta}} \tag{8}$$

$$i_{\beta}^* = \frac{2}{3}\frac{q^*\psi_{g\beta} + T_v^*u_{g\beta}}{u_{g\beta}\psi_{g\alpha} - u_{g\alpha}\psi_{g\beta}} \tag{9}$$

It can be found in [32] dedicated to DFIG, that fixed both electromagnetic torque and $q$ component of instantaneous stator power are associated with sinusoidal (nonetheless unbalanced) current with asymmetry accorded to the grid voltage asymmetry, that means assumed basic target for rectifier mode. Provided that the torque is constant, only constant $q$ component causes no high harmonics of the stator current. The case with active rectifier is analogous.

DC link circuit equation can be derived from (4) and (5).

$$\frac{du_{dc}}{dt} = \frac{3}{2C_{dc}}\frac{\left(u_{g\alpha}i_{\alpha} + u_{g\beta}i_{\beta}\right)}{u_{dc}} - \frac{1}{C_{dc}}i_{ld} \tag{10}$$

Taking into account equations (8)(9), there can be derived dependence of DC link voltage (11) on the reference virtual torque $T_v^*$ and $q^*$ component of instantaneous power.

$$\frac{du_{dc}}{dt} = \frac{T_v^*}{C_{dc}u_{dc}}\frac{\left(u_{g\alpha}^2 + u_{g\beta}^2\right)}{\left(u_{g\beta}\psi_{g\alpha} - u_{g\alpha}\psi_{g\beta}\right)} + \\ + \frac{q^*}{C_{dc}u_{dc}}\frac{\left(u_{g\alpha}\psi_{g\alpha} + u_{g\beta}\psi_{g\beta}\right)}{\left(u_{g\beta}\psi_{g\alpha} - u_{g\alpha}\psi_{g\beta}\right)} - \frac{1}{C_{dc}}i_{ld} \tag{11}$$

Finally, the reference virtual torque can be derived as the function of required DC link voltage, but this dependence is influenced by load current $i_{ld}$ treated as disturbance and reference $q^*$ component of instantaneous power as the coupling from parallel control path. It can be seen that model is nonlinear and to keep fixed gain of the DC link voltage controller, regulator output has to be normalized using a function dependent on the grid voltage imbalance.

$$T_v^* = \frac{C_{dc}}{u_{dc}}\frac{\left(u_{dc}^* - u_{dc}\right)}{T_s}\frac{\left(u_{g\beta}\psi_{g\alpha} - u_{g\alpha}\psi_{g\beta}\right)}{\left(u_{g\alpha}^2 + u_{g\beta}^2\right)} + \\ - q^*\frac{\left(u_{g\alpha}\psi_{g\alpha} + u_{g\beta}\psi_{g\beta}\right)}{\left(u_{g\alpha}^2 + u_{g\beta}^2\right)} + \frac{1}{C_{dc}u_{dc}}i_{ld}\frac{\left(u_{g\beta}\psi_{g\alpha} - u_{g\alpha}\psi_{g\beta}\right)}{\left(u_{g\alpha}^2 + u_{g\beta}^2\right)} \tag{12}$$

Referencing $q$ component of power and treating the load current as a disturbance, it can be created the control structure of DC link voltage, as it is shown in Fig. 7. Such a structure is able to eliminate the DC link voltage oscillations analogously to the fixed $p$ component case. In fact, this is a variant of fixed $p$ component reference. However, it does not allow to keep sinusoidal current when both $p$ and $q$ components of power are fixed. Introduction of adequate $q$ power component pulsation providing sinusoidal unbalanced current does not allow to reach assumed target for active rectifier, which is the highest current in the phase with the highest voltage.

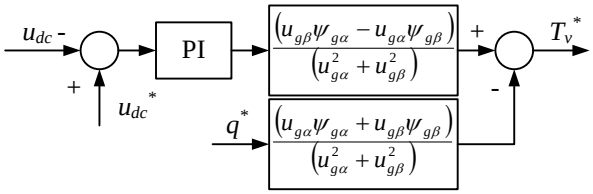


Fig. 7. The DC link voltage control with consideration of coupling term from $q$ power component and with consideration of model gain variation compensation according to the grid voltage asymmetry.

Simulation results of active rectifier with 1.4kW step unloading at 0.4s and step loading at 0.5s with simultaneous -0.5kVA of $q$ power during grid voltage asymmetry is presented in Fig. 8. The DC link voltage control structure giving fixed $p$ and $q$ power components have been applied. Additionally, the grid voltage is distorted by 10V of 5$^{th}$ and 10V of 7$^{th}$ harmonics. The converter current is strongly nonlinear, and this is unwanted target for active rectifier. These results are made to show that derived model is correct, but finally the control must be modified to obtain sinusoidal currents. In order to obtain effects, that is sinusoidal phase current, all oscillatory components have to be removed from the controlled variables $T_v$, $q$, and $u_{dc}$. The final proposed control structure for virtual torque and $q$ component of instantaneous power is shown in Fig. 9. The average of reference $q$ component is set to zero for rectifier operation, therefore the decoupling from $q$ component in this structure is omitted. The signal produced by DC link voltage control structure in Fig. 7 has oscillatory component due to additional term depending on the grid voltage asymmetry. Due to the wanted constant value of reference virtual torque $T_v^*$ providing sinusoidal unbalanced converter current the nonlinear term behind the voltage controller is also removed.

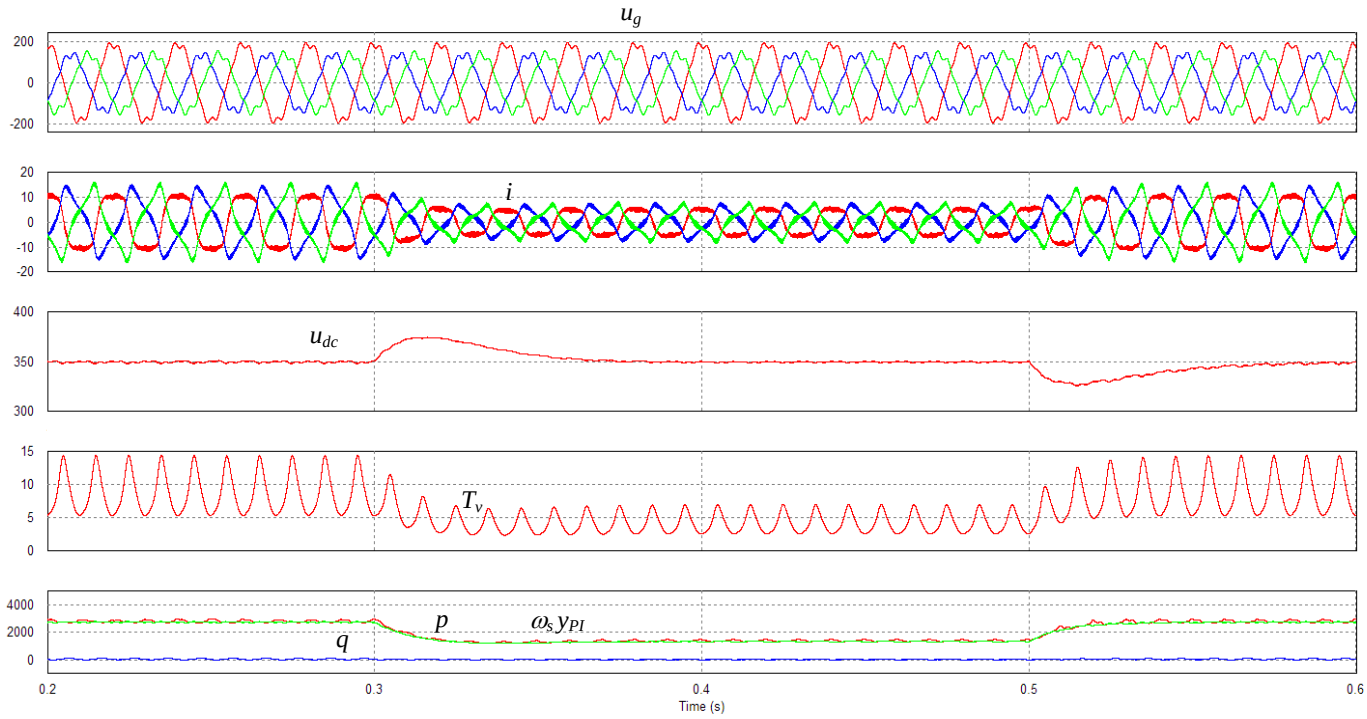


Fig. 8. Simulation results of converter operating with grid voltage asymmetry and harmonics - grid voltage $u_g$, DC voltage $u_{dc}$, converter current $i$, virtual torque $T_v$, and $pq$ power components.

This way the DC link voltage controller can be tuned as for symmetrical grid, for which the nonlinear term behind DC voltage controller from Fig. 7 equals grid voltage pulsation $\omega_s$. This means, that the output signal from PI controller is responsible for average of $p$ component of power, and the PI controller is tuned in the same manner like in the Direct Power Control with Space Vector Modulation (DPC-SVM) at symmetrical grid. Simultaneously, the measured DC voltage is filtered in the same way as presented in Fig. 2.

Fig. 10 presents the simulation results for the same conditions as in the simulation tests that are presented in Fig. 8, but with the use of the control from Fig. 9, that means with filtration of measured DC voltage and without nonlinear terms from Fig. 7 in the DC voltage control path. In this case, the current is sinusoidal, and its hodograph is a scaled version of the grid voltage hodograph created by fundamental frequency voltage vector components in $\alpha\beta$ frame.

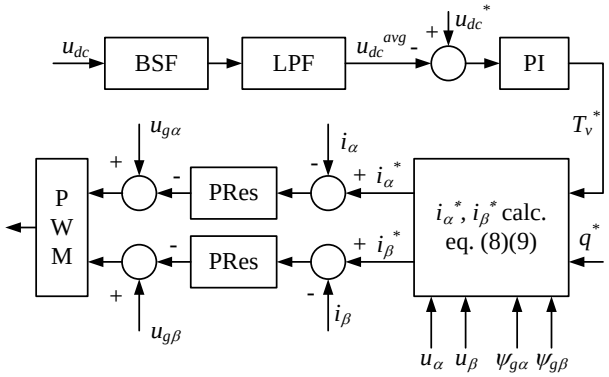


Fig. 9. The proposed method main structure of current control for sinusoidal unbalanced current target of active rectifier at unbalanced grid conditions based on virtual torque concept.

The current harmonics content is negligible. The $p$ power component oscillations contains not only 100Hz component related to the voltage and current asymmetry, but also 300Hz component related to the 5th and 7th harmonics of grid voltage. During unbalanced grid operation, it is not possible to deliver the rated power without exceeding the phase current limit. Sinusoidal balanced current provides higher average value of $p$ power component (higher active power calculated by definition), so more energy can be transferred from the grid to DC link. Thus, there are required two additional algorithms for the current control method from Fig. 9. The first one is current limitation, and the second one is balancing of current to deliver more energy to the DC link when unbalanced current reaches maximum value at least in one phase.

### C. *Progressive balancing of the converter current (smooth change of targets)*

The balancing of converter current can be made by progressive reduction (up to full elimination) of double grid frequency oscillations in the reference current components transformed to the $dq$ frame. The damping factor $\xi$ of band-stop filter BSF responsible for reduction of double grid frequency pulsation is provided by external algorithm, which detects the moment when the converter reaches current limit.

The bandwidth of BSF can be set on 10Hz around 100Hz to eliminate oscillations of $dq$ current components even in case of grid frequency deviation from 50Hz. The angular speed of $dq$ frame rotation should be set at expected grid voltage frequency $\omega_s$. However, it is not necessary to synchronize this frame with any grid variable, like voltage or virtual flux, because it is used only to eliminate unwanted oscillatory component, and the control is designed in $\alpha\beta$ stationary frame.

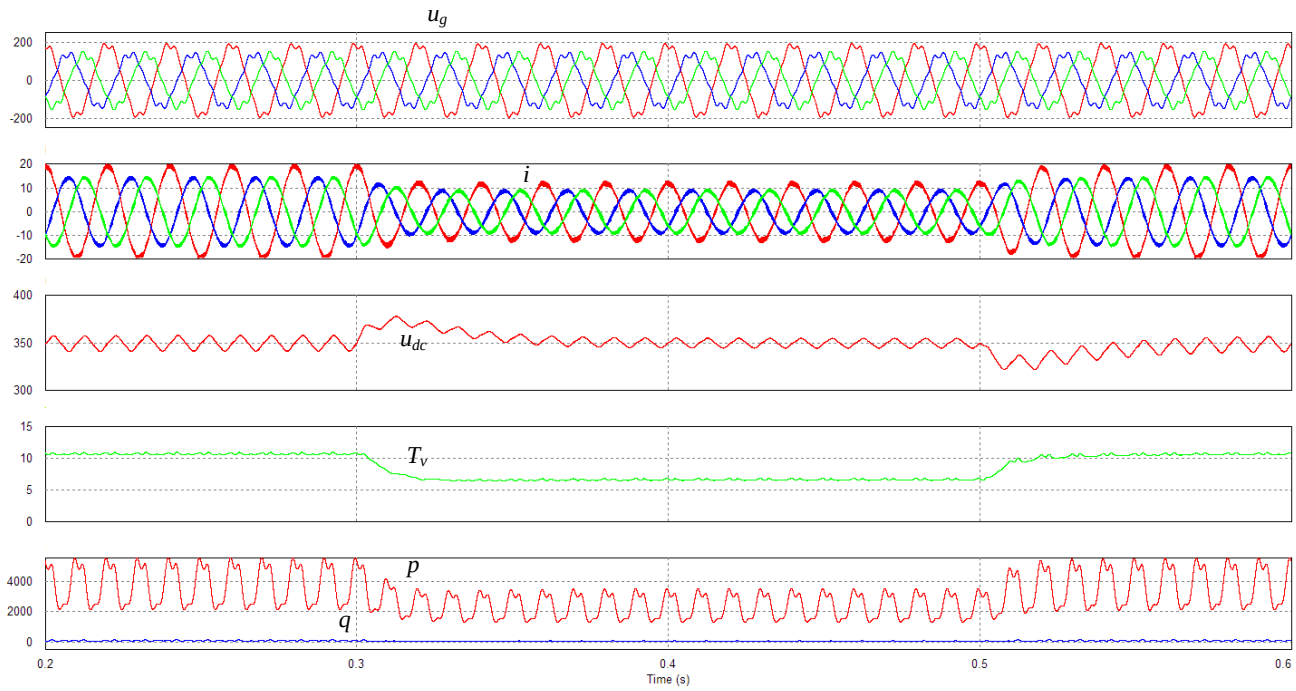


Fig. 10. Simulation results of converter operating with grid voltage asymmetry and harmonics - grid voltage $u_g$, DC voltage $u_{dc}$, converter current $i$, virtual torque $T_v$, and $pq$ power components.

The new reference values of converter current components in $\alpha\beta$ frame $i_{\alpha new}^*$, $i_{\beta new}^*$ are obtained by inverse transformation of modified $dq$ components to $\alpha\beta$ frame with the same angle that is used for transformation from $\alpha\beta$ to $dq$ frame (Fig. 11).

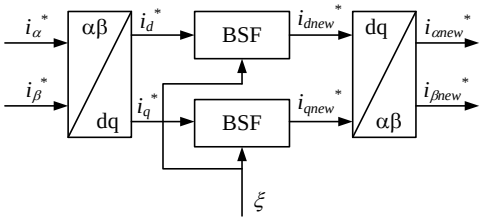


Fig. 11. The method of converter current balancing using adaptive band-stop filters reducing oscillatory terms of $dq$ reference current components.

### D. Converter current limitation

Typical current limitation methods use sequence decomposition. When the current limitation is based on reduction of the current vector length, the complication level of the structure is not very high (Fig. 2). However, simple limitation of current vector magnitude does not mean that phase currents reach their maximum rms values. Therefore more sophisticated methods (also based on sequence decomposition) are proposed. However, the complexity of these new methods permitting real phase current limitation is significant [16][20].

The proposed structure of phase current limitation (Fig. 12) does not require complicated calculation based on positive and negative sequences, but it bases on separate limitation of three phase signals of reference current, obtained from the progressive balancing structure from Fig. 11. In order to do that, first of all, the new reference signals $i_{\alpha new}^*$, $i_{\beta new}^*$ from Fig. 11 are transformed to $abc$ frame to obtain separate signals of reference phase currents $i_{anew}^*$, $i_{bnew}^*$, $i_{cnew}^*$ (Fig. 12). Next, separate PLL structures for each phase are used to find out normalized signals $i_{aunit}^*$, $i_{bunit}^*$, $i_{cunit}^*$, which multiplied by assumed current limit $|i|^{limit}$ give the sinusoidal waveforms of maximum current $i_{alimit}^*$, $i_{blimit}^*$, $i_{climit}^*$ in each phase. It has to be noted that sinusoidal signals of phase current limitation are always synchronized with new reference signals $i_{anew}^*$, $i_{bnew}^*$, $i_{cnew}^*$ obtained from the progressive current balancing blocks, independently of the reference current symmetry or asymmetry. The absolute values of new references $i_{anew}^*$, $i_{bnew}^*$, $i_{cnew}^*$ obtained from balancing block are compared with absolute values of the limitation signals $i_a^{limit}$, $i_b^{limit}$, $i_c^{limit}$ in each phase separately in order to indicate whether the phase current exceeds the limit or not.

The error is integrated to change the damping factor $\xi_x$ (in the range from zero to one) in each phase respectively. Finally the highest value among the phase damping factors is chosen to modify damping factor $\xi$ of band-pass filters from Fig. 11. The damping factor different from zero means current limitation exceeding in respective phase. Finally referenced $abc$ currents can be chosen from $i_{anew}^*$, $i_{bnew}^*$, $i_{cnew}^*$ and $i_a^{limit}$, $i_b^{limit}$, $i_c^{limit}$ for each phase separately depending on the reference current exceeding limits or not. However, in order to avoid unwanted switching between respective signals in transients and to avoid hysteresis structure used for switching between respective signals, the final references $i_{anew2}^*$, $i_{bnew2}^*$, $i_{cnew2}^*$ are calculated based on both reference phase current $i_{xnew}^*$ and current limitation $i_x^{limit}$ according to (13).

$$i_{xnew2}^* = \xi_x i_x^{limit} + (1-\xi_x) i_{xnew}^* \tag{13}$$

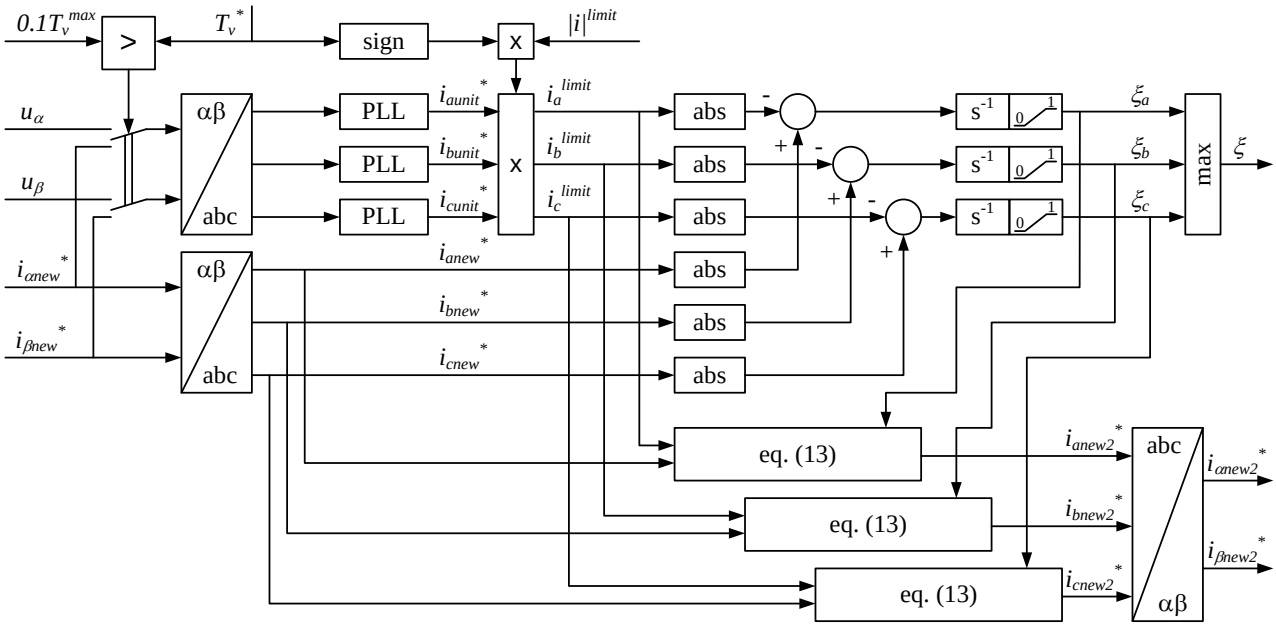


Fig. 12. The proposed method of converter current limitation in both assumed targets and during intermediary states without signals decomposition.

### *E. Synchronization at low reference current*

Some problem in the proposed method of phase current limitation may occur when the converter operates under no-load conditions. Then, originally calculated reference currents $i_a^*$, $i_b^*$, $i_c^*$ are close to zero (only losses are covered). Further, the reference current signals are not modified by current balancing block due to the current much below the limit, and such low signals cannot be used by PLL structures for synchronization of current limitation signals with reference ones. As the system is developed for active rectifier, and it is assumed that reference $q^*$ component of power equals zero, the reference unbalanced current (main target) is synchronized with the grid voltage.

Thus, below some arbitrarily set torque level (here when reference torque obtained from DC link voltage PI controller is less than 10% of maximum virtual torque) the input signals for PLL blocks are the signals of the phase voltage instead of reference current. This way, the current limitation signals are still sinusoidal and they are ready to be compared with the reference current even in case of step loading and rapid increase of the reference phase current. It prevents of losing the proper phase by current limitation signal and shortens seeking of these signals proper phase after step loading causing excess of the phase current limit.

During negative current flow in case of transient under-voltage in DC link caused by step unloading, the phase of current limit signals $i_a^{limit}$, $i_b^{limit}$, $i_c^{limit}$ are changed to counter-phase by consideration of virtual torque sign at $|i|^{limit}$ value. This is done to avoid resynchronization of current limit signals to opposite sine wave during short time of inverter operation at DC overvoltage after step unloading. The described manner does not change anything in operation of overcurrent detection method, as it is made by comparison of absolute values of actual current and calculated limitation signal in each phase respectively.

The introduced selection of the input variable for synchronization block depending on the reference virtual torque level can be made only for reference *q* component equal zero, as it is assumed typically for active rectifiers. For other converters (grid inverters in generating systems and active filters) the reference current may have other phase than the grid voltage under non-zero *q* power. However, for these other cases, not only synchronization part, but the whole control structure should be changed. However, it is out of the paper scope and will be developed in future.

## IV. Laboratory and Simulation Results

### *A. Laboratory test bench and overall control system*

The parameters of active power rectifier are presented in the Table 1. The converter is connected to the transformer giving nominally 3x230V line-to-line rms symmetrical voltage. Assumed 15A of phase current amplitude determines the maximum power equal to 4.25kW (at rated grid voltage). The block diagram of proposed control system verified in the laboratory tests is presented in Fig. 13. It includes the blocks such as virtual torque based control, grid voltage and flux vectors components calculation, current balancing, phase current limitation, and current control based on proportional-resonant terms.

TABLE I
Parameters of Active Rectifier Used in Laboratory Unit

| Symbol | Parameter | Values |
|---|---|---|
| $P_n$ | Rated power | 4.25kW |
| $U_{gn}$ | Nominal grid voltage (L-L rms) | 230V |
| $I_{gn}$ | Rated current amplitude | 15A |
| $L$ | Grid filter inductance | 1.2mH |
| $R_L$ | Inductor resistance | 40mΩ |
| $L_T$ | Transformer leakage inductance | 2.3mH |
| $C_{dc}$ | DC link capacitance | 1mF |
| $U_{dc}$ | Reference DC voltage | 350V |
| $f_s$ | Switching frequency | 4kHz |

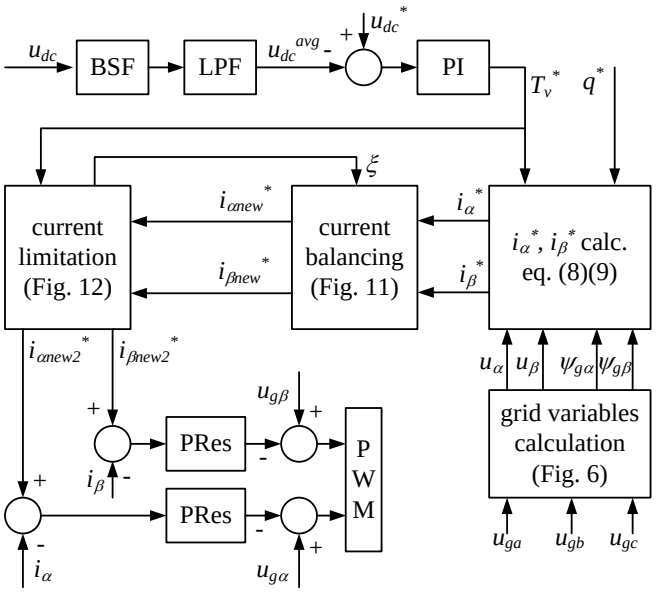


Fig. 13. The proposed control method with main parts - virtual torque control, grid voltage and flux vector components calculation, current progressive balancing, true phase current limitation, and resonant controllers based current vector components control in the stationary frame.

### B. *Steady states*

Fig. 14 presents simulation (Fig. 14a) and laboratory (Fig. 14b) tests results of active rectifier operated at unbalanced power grid, when the load power equals 1.4kW, that is around half of the power possible to be supplied under this voltage asymmetry (2.8kW at asymmetrical current with asymmetry accorded to the grid voltage asymmetry, and 3.1kW at symmetrical current). Converter current asymmetry in these tests (Fig. 14) is in accordance to the voltage asymmetry, what causes fixed virtual torque $T_v$ (4Nm) and $q$ (0kVA) component of instantaneous power, as well as significant oscillations of $p$ component of power with 1.4kW of average value. Fig. 15 presents three phase converter current at the same grid voltage conditions registered by another four channel recorder equipped with FFT function (Fig. 15b) and from simulation (Fig. 15a), when the current reaches maximum value 15A in one phase. It can be seen in both simulation and experimental tests that main current distortion is caused by 4kHz switching frequency component, while other harmonics occurred in experiment are negligible (less than harmonics caused by switching). Besides the grid voltage imbalance, it can be seen some content of higher harmonics, with total THD factor 3% (with consideration of switching frequency harmonics) and 0.7% (without switching frequency harmonics, which can be removed by the use of LCL filter instead of single inductor used in the experiment). The influence of grid voltage harmonics on the converter current is insignificant in the proposed control of converter current.

Fig. 16 presents the case of symmetrical sinusoidal converter current during current limitation. Current amplitude reaches the limited value set to 15A what corresponds to 9Nm of average virtual torque and 3.1kW of average value of $p$ component of instantaneous power. For this case, the load has been chosen slightly higher than the one for which a reference 350V of DC link voltage can be achieved. This is to show that the current limitation in all phases works correctly as the final stage of progressive balancing.

Symmetrical current is the case of maximum average value of $p$ component of power (definition of active power) limiting the energy transfer to the DC link. However, even there the DC voltage drops, when transferred power is lower than the power required by DC load at reference DC voltage. Further increase of the DC load power (decrease of load resistance) will cause larger DC voltage drop and may need switching off of the power converter and its disconnection from the grid to avoid uncontrolled current flow.

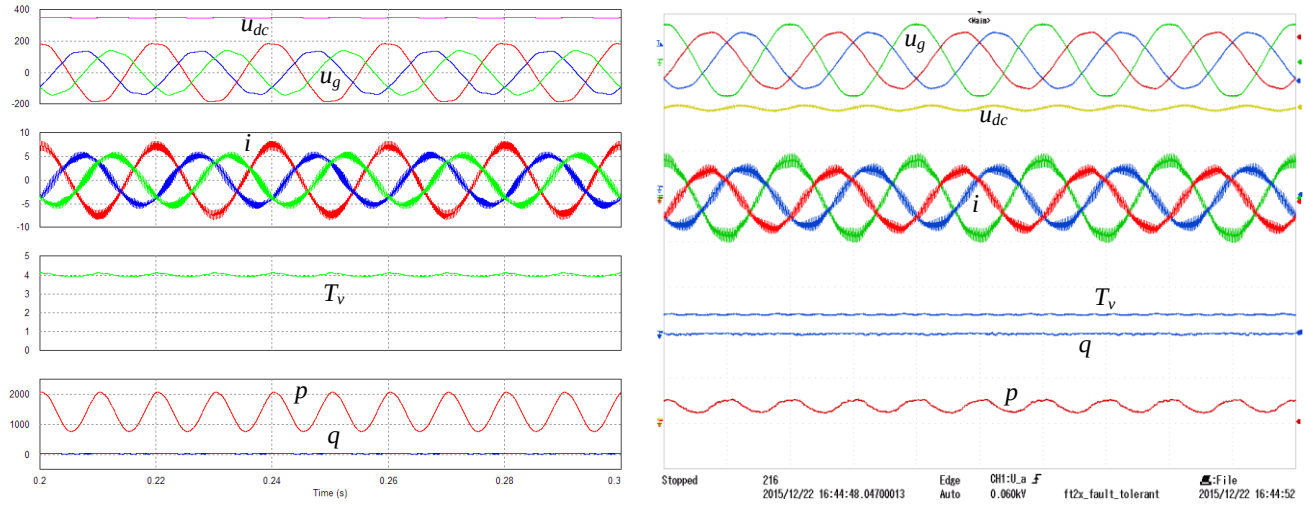


(a) (b)

Fig. 14. Oscillograms presenting the case of constant virtual torque and reactive power target, a) simulation, b) experiment - grid voltage $u_g$ (250V/div), DC voltage $u_{dc}$ (50V/div), converter current $i$ (10A/div), virtual torque $T_v$ (10Nm/div), and $pq$ power components (4kW/div).

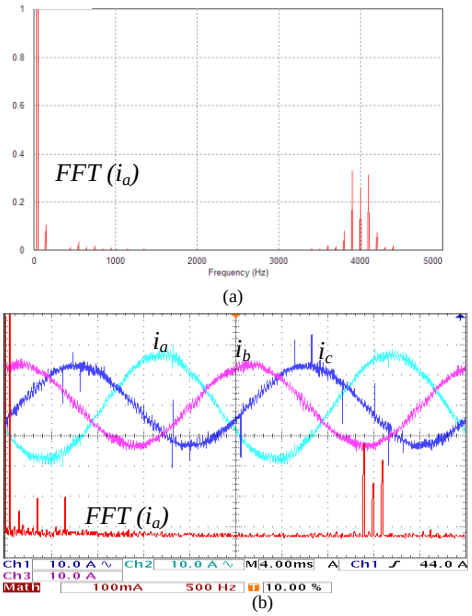


Fig. 15. Oscillograms presenting FFT spectrum of converter current at fixed virtual torque and reactive power target in a) simulation, and b) experiment - (100mA/div for FFT, and 10A/div for current waveforms).

It has to be noted that stable operation was possible with lower DC voltage due to the constant resistance load consuming less energy at lower voltage. In the case of constant power load type, the DC voltage will successively drop and at some level the system must be switched off due to the uncontrolled converter current below some DC voltage level. But in some systems (e.g. pumps or fans driven by power converter drives) we can decrease the consumed power by reduction of speed, which implicates reduction of pressure/flow and consequently reduction of consumed power.

However, the load management in this case is quite trivial and is limited to the reduction of the machine electromagnetic torque, depending on the DC voltage drop. Operation with current limitation in all phases causes that reference DC link voltage cannot be reached, and in this particular case, the DC voltage drops to 330V (average value). Symmetrical current target causes oscillations of all three variables – virtual torque, and *pq* instantaneous power components. In both cases (from Fig. 14 and 16) the DC voltage has visible 100Hz oscillations, due to oscillatory character of *p* component of instantaneous power. This is why unbalanced grid operation compliance with the proposed symmetrical current target as a final state of current progressive balancing may require larger DC link capacitance than under operation with balanced grid to reduce the voltage oscillations if needed by the supplied load.

Fig. 17 presents the case of over-current protection realized as limitation of the instantaneous length of current vector creating originally elliptical hodograph, which exceeds the circular hodograph representing maximum balanced current. It is visible that this method introduces high content of higher harmonics in all phase currents and it is not adequate for application. Increasing the load power, the current hodograph will be more circular and the phase currents become less distorted. Second method compared with proposal is presented in Fig. 18. The elliptical hodograph exceeding the hexagon is cut by the hexagon lines. This makes limitation of the instantaneous value of the phase current. The current with higher amplitude is naturally saturated first, while the other phase currents will be increased by the DC voltage controller. Finally, the phase currents will be symmetrical, but trapezoid. Thus, it is a variant of the method with progressive balancing with non-sinusoidal phase current.

The last case tested is a basic part of control without progressive balancing and without current limitation (removed two blocks from Fig. 13). Due to the lack of current limitation, the DC link voltage can be kept at reference value. However, some phase currents may exceed their maximum rms values (Fig. 19). There is also possible a variant of progressive balancing without current limitation. It will cause initially progressive balancing of phase current up to full symmetry, and further equable increase of all phase currents over the limit when the current demanded by DC voltage regulator will increase to keep the DC voltage at reference value.

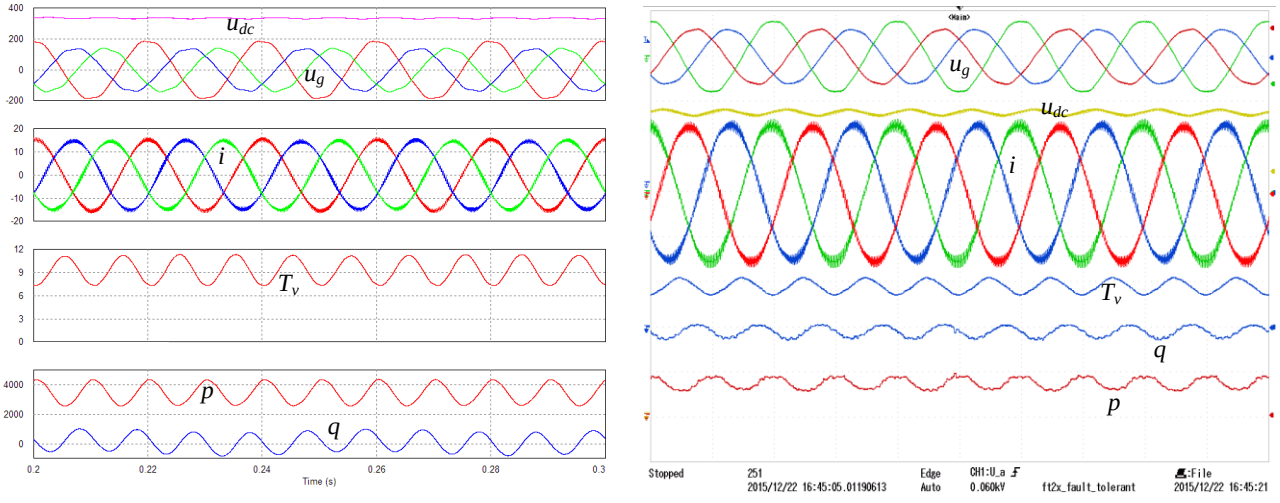


Fig. 16. Oscillograms presenting the case of limited balanced current, a) simulation, b) experiment - grid voltage $u_g$ (250V/div), DC voltage $u_{dc}$ (50V/div), converter current $i$ (10A/div), virtual torque $T_v$ (10Nm/div), and *pq* power components (4kW/div).

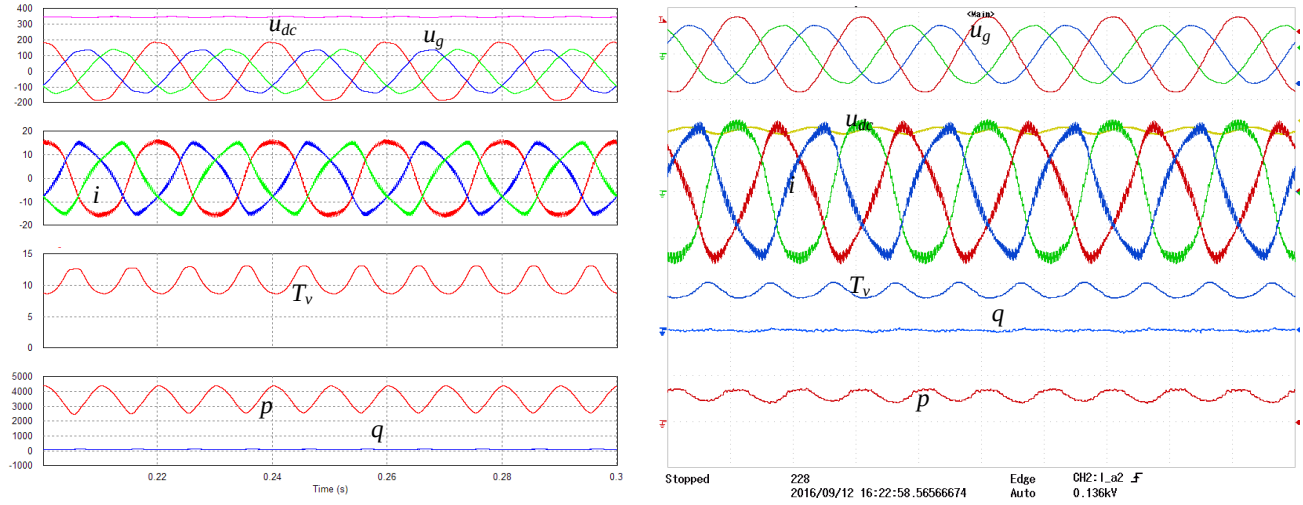


(a) (b)

Fig. 17. Oscillograms presenting the case of current vector instantaneous length limitation, a) simulation, b) experiment - grid voltage $u_g$ (250V/div), DC voltage $u_{dc}$ (50V/div), converter current $i$ (10A/div), virtual torque $T_v$ (10Nm/div), and $pq$ power components (4kW/div).

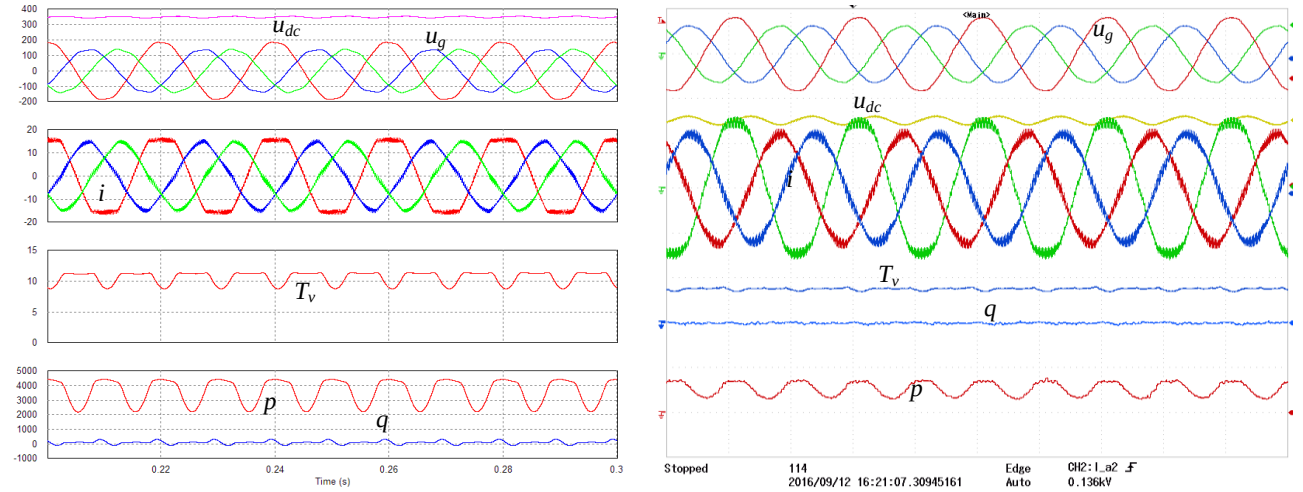


(a) (b)

Fig. 18. Oscillograms presenting the case of limitation of phase current instantaneous value, a) simulation, b) experiment - grid voltage $u_g$ (250V/div), DC voltage $u_{dc}$ (50V/div), converter current $i$ (10A/div), virtual torque $T_v$ (10Nm/div), and $pq$ power components (4kW/div).

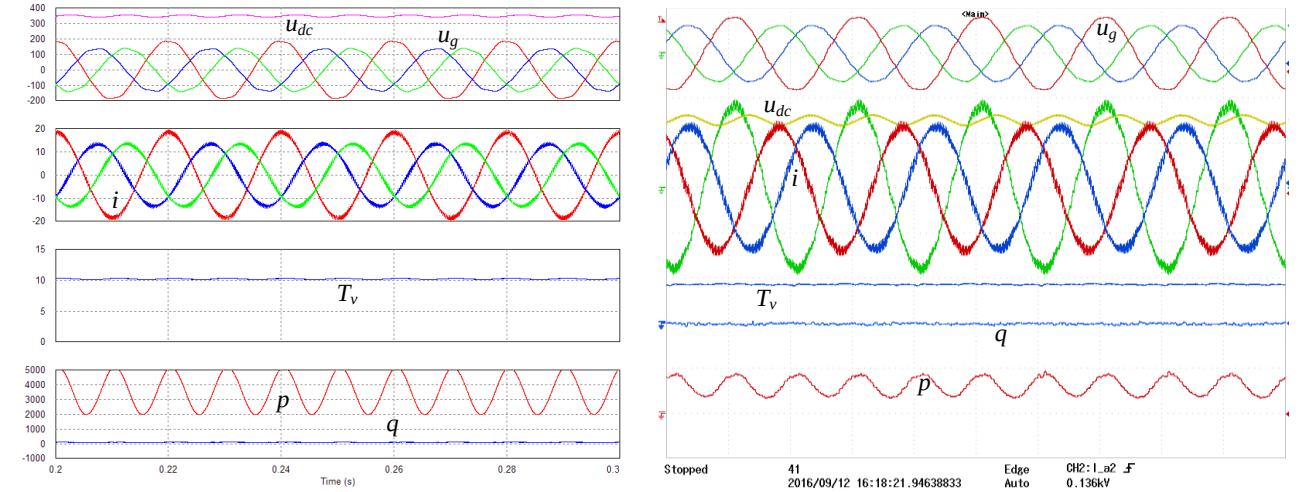


(a) (b)

Fig. 19. Oscillograms presenting the case of no progressive balancing and without current limitation, a) simulation, b) experiment - grid voltage $u_g$ (250V/div), DC voltage $u_{dc}$ (50V/div), converter current $i$ (10A/div), virtual torque $T_v$ (10Nm/div), and $pq$ power components (4kW/div).

### C. *Transient states caused by step loading and unloading*

Fig. 20 presents transient state caused by step loading (3.1kW) during which, it is required maximal current in all three phases. It can be seen, that after load step change, the DC link voltage cannot reach reference value. Further increase the load power will deepen DC voltage drop and it will be required to switch off the system and to disconnect it from power grid. However, the system response is fast and initially (during first two periods after step loading) converter current is being successively balanced. Fig. 21 shows transient caused by step loading (more less half of load possible to be supplied at assumed grid voltage imbalance - 1.4kW), for which the target of fixed virtual torque and $q$ component of instantaneous power is possible. Next, additional step loading (3.1kW of total power) requires symmetrical converter current at limited level in all phases. The current changes fast from unbalanced to balanced.

Fig. 22 presents transient caused by step unloading from the load power 3.1kW (requiring full current in all three phases), to zero. It can be seen that the DC link voltage reaches reference value after short overregulation due to unloading. Instantly, the reference virtual torque is negative to allow DC link energy surplus return to the grid. Fig. 23 presents transient caused by step partial unloading (from full power 3.1kW to 1.4kW), and next, additional step unloading from 1.4kW to zero. The current changes fast from balanced to unbalanced. Progressive balancing of converter current is shown in Fig. 24, presenting simulation tests at the same voltage asymmetry as in previous simulations and experiments. The variable load has been simulated as a DC connected controlled current source with the current value changed from zero to 10A. This is another type of load than in previous tests, because the load power changes proportionally to the DC voltage, whereas in the case of constant resistance the power changes with the square of voltage. However, it does not change the converter behavior in terms of current limitation and progressive balancing in the case in which the load power at reference DC voltage exceeds the value of maximum power at given grid voltage asymmetry.

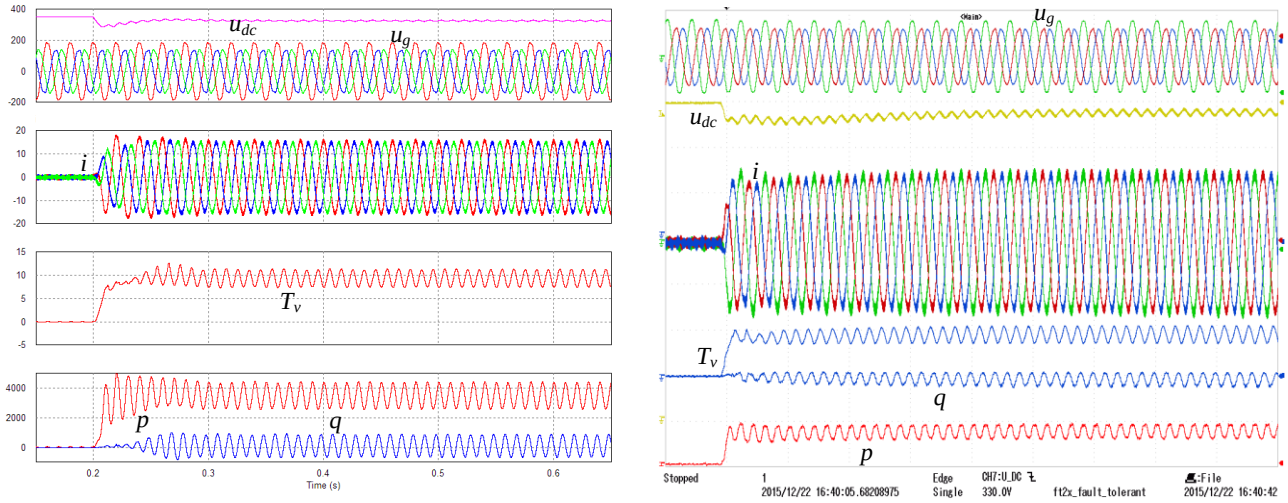


(a) (b)

Fig. 20. Oscillograms presenting the transient after full loading (3.1kW), a) simulation, b) experiment - grid voltage $u_g$ (250V/div), DC voltage $u_{dc}$ (50V/div), converter current $i$ (10A/div), virtual torque $T_v$ (10Nm/div), and $pq$ power components (4kW/div).

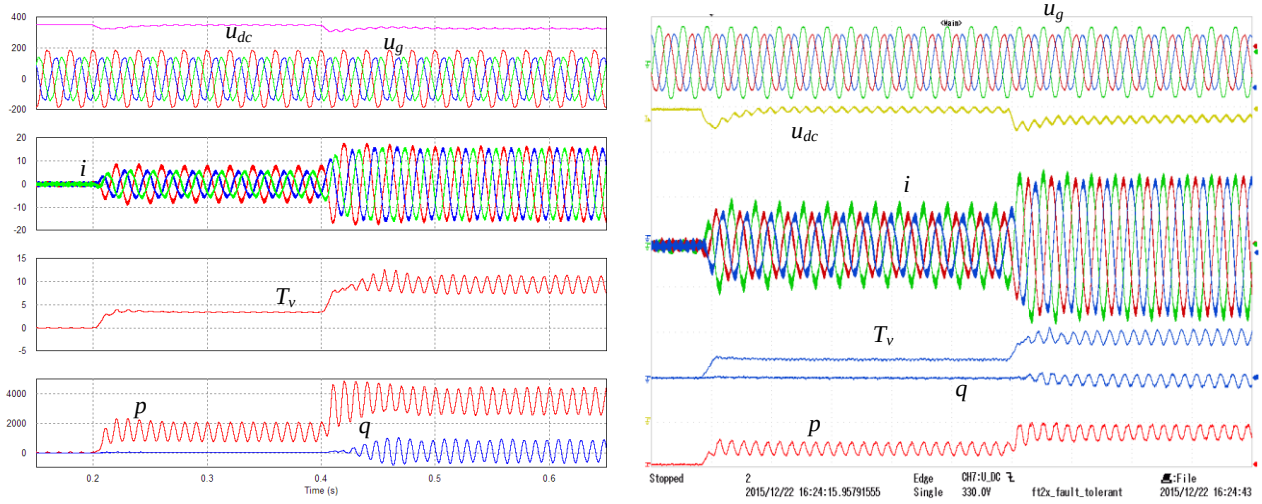


(a) (b)

Fig. 21.Oscillograms presenting the transient after step partial loading (1.4kW) and full loading (3.1kW), a) simulation, b) experiment - grid voltage $u_g$ (250V/div), DC voltage $u_{dc}$ (50V/div), converter current $i$ (10A/div), virtual torque $T_v$ (10Nm/div), and $pq$ power components (4kW/div).

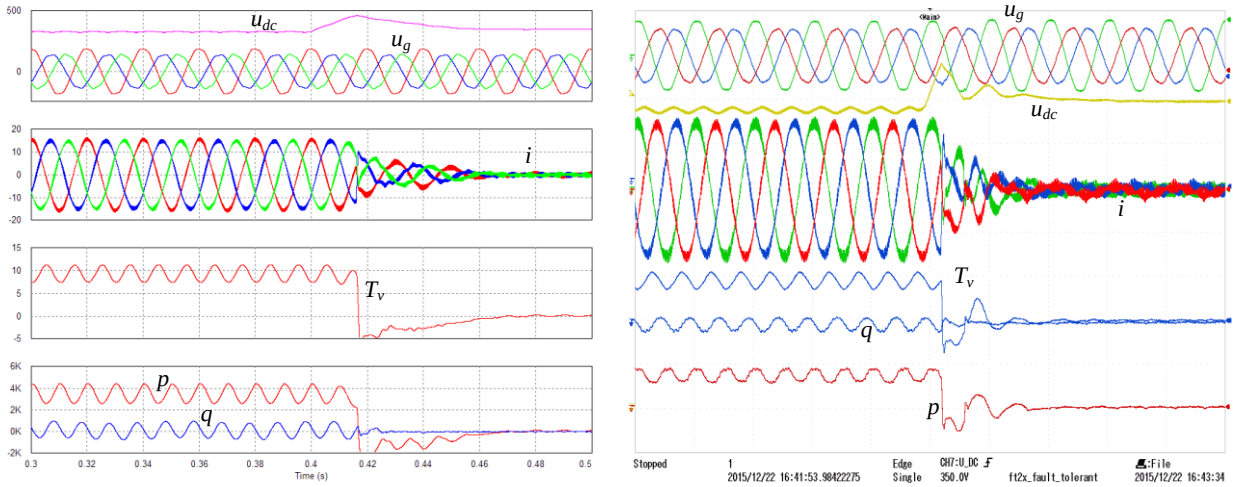


(a) (b)

Fig. 22. Oscillograms presenting the transient after step unloading from 3.1kW to zero, a) simulation, b) experiment - grid voltage $u_g$ (250V/div), DC voltage $u_{dc}$ (50V/div), converter current $i$ (10A/div), virtual torque $T_v$ (10Nm/div), and $pq$ power components (4kW/div).

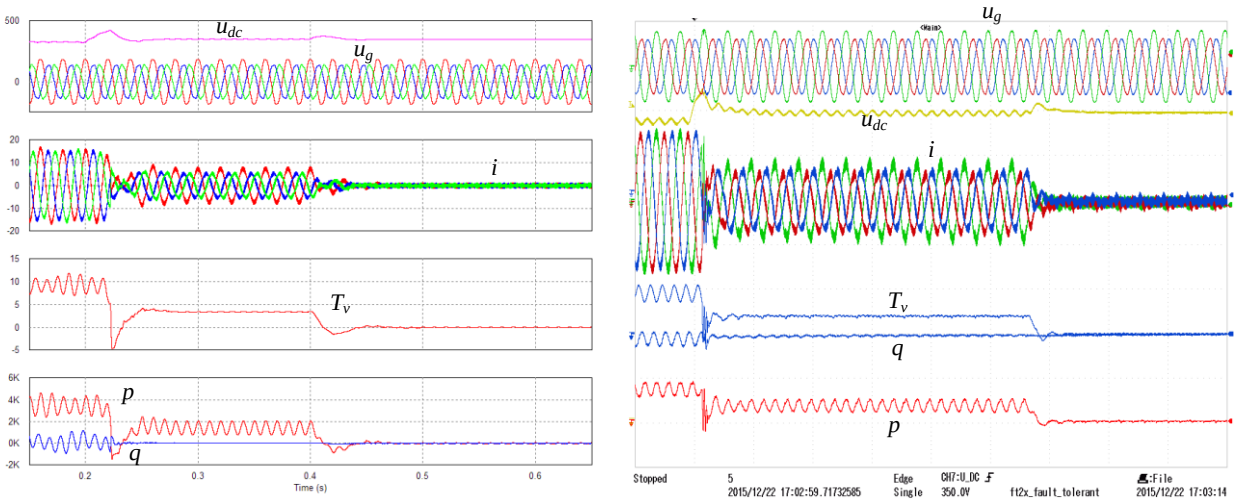


(a) (b)

Fig. 23. Oscillograms presenting the transient after unloading from 3.1kW to 1.4kW, and from 1.4kW to zero, a) simulation, b) experiment - grid voltage $u_g$ (250V/div), DC voltage $u_{dc}$ (50V/div), converter current $i$ (10A/div), virtual torque $T_v$ (10Nm/div), and $pq$ power components (4kW/div).

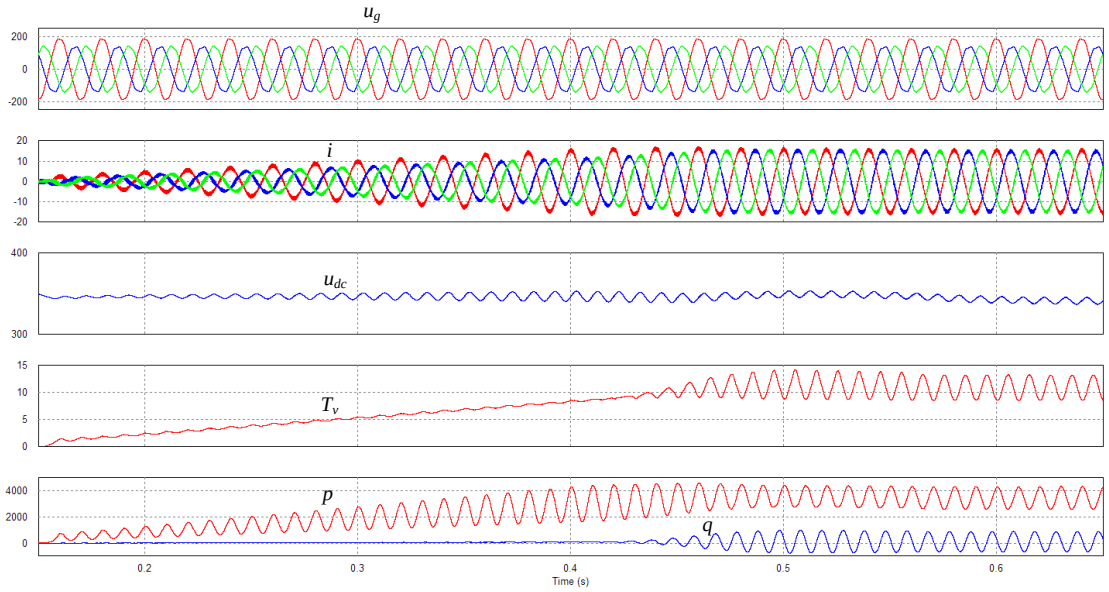


Fig. 24. Oscillograms presenting the transient of progressive current balancing during load current increase from zero to maximum - grid voltage $u_g$, DC voltage $u_{dc}$, converter current $i$, virtual torque $T_v$, and $pq$ power components.

### D. *Transient states caused by asymmetrical voltage sag*

Due to the inability to generate grid voltage sag in a laboratory unit, they have been done simulation tests only. Fig. 25 presents the operation during two phase grid voltage sag in the time period from 0.2s to 0.4s. Despite the grid voltage harmonics, converter current is sinusoidal. The required power is lower than nominal one and converter current is lower than its limit under symmetrical grid voltage conditions. DC voltage and all variables, such as virtual torque $T_v$, and $pq$ power components, are constant. After the voltage sag the converter current reaches imbalance in accordance to grid voltage imbalance to achieve unity power factor in each phase. For such a condition, the DC voltage oscillations are produced, but the average value is obtained on the reference level. Except short transients the electromagnetic torque is almost free of oscillations, similarly to the $q$ component of instantaneous power. Expected oscillations of $p$ component of instantaneous power occur, but its average value (active power) is maintained on the same level as before and after grid voltage sag. It means the energy consumption does not change as the load power is constant. Faster response is possible, but it requires to resign of the low-pass filter making possible filtration of oscillations in a measured DC voltage. However, the system is sensitive to grid voltage harmonics. Registration of waveforms with higher content of grid voltage harmonics was impossible in the laboratory unit, but the simulation results shown in Fig. 25 with high amount of grid voltage harmonics proves that sinusoidal current can be obtained for higher THD factors too.

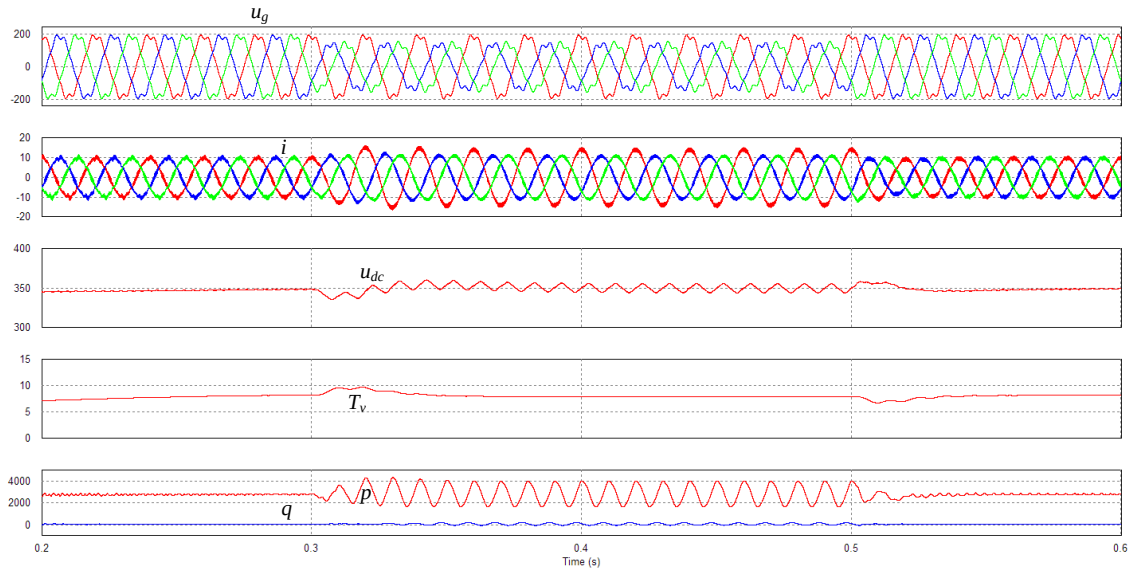


Fig. 25. Oscillograms presenting the transient of distorted grid voltage asymmetrical sag - grid voltage $u_g$, DC voltage $u_{dc}$, converter current $i$, virtual torque $T_v$, and $pq$ power components.

## V. Conclusion

The proposed control method of three-phase active rectifier bases on the virtual torque of power network treated as virtual machine. The proposed control allows progressive change of targets from unbalanced converter current (fixed virtual torque and $q$ component of reactive power) to symmetrical current necessary when supplied load power demands high power. The phase current limitation method works for both targets and in intermediary states. Current limitation is obtained through determination of unity signals in phase with reference phase currents by single phase PLL structures. The system is protected against the problems with synchronization with reference current for low reference current values. All simulation tests and experiments confirm that the control system has good dynamic properties, whereas the calculation procedure of reference current is simpler than usually used methods based on sequence decomposition. Progressive change of converter current asymmetry is obtained by filtration of $dq$ current vector components oscillations by adaptive band-stop filter. The method is dedicated for active rectifier, for which the reference signal of instantaneous power $q$ component equals zero. The proposed current limitation method giving sinusoidal phase current in the limitation region has been compared with the methods typical for balanced current targets, giving non-sinusoidal phase current in the limitation region when unbalanced current is referenced. The future work will be concentrated on extension of the proposed method to inverter operation mode for power generating systems feeding the energy to the unbalanced grid, which is important issue for renewable energy sources.

## References

[1] L. Malesani and P. Tenti, "A novel hysteresis control method for current controlled VSI PWM inverters with constant modulation frequency," *IEEE Trans. Ind. Appl.*, vol. 26, pp. 88–92, Jan./Feb. 1990.

[2] Q. Yao and D. G. Holmes, "A simple, novel method for variable-hysteresis-band current control of a three phase inverter with constant switching frequency," *Conf. Rec. IEEE-IAS Annu. Meeting*, Toronto, Ont., Canada, Oct. 1993, pp. 1122–1129

[3] T. Noguchi, H. Tomiki, S. Kondo, I. Takahashi, "Direct Power Control of PWM converter without power-source voltage sensors., *IEEE Trans. on Ind. Applications*, vol. 34, no. 3, pp. 473-479, May/June 1998.

[4] T. Ohnishi "Three-phase PWM converter/inverter by means of instantaneous active and reactive power control", *Ind. Electron. Conf. – IECON'91*, Kobe, Japan, 1991, pp. 819-824,

[5] C. T. Rim, et al., "A complete DC and AC analysis of three-phase controlled-current PWM rectifier using circuit D-Q transformation," *IEEE Trans. Power Electron.*, vol. 9, pp. 390–396, July 1994.

[6] N. R. Zargari and G. Joos, "Performance investigation of a current-controlled voltage-regulated PWM rectifier in rotating and stationary frames," *Int. Conf. on Industrial Electronics, Control and Instrumentation–IECON'93,* Maui, Hawai, USA, 1993, pp. 1193–119,

[7] M. Malinowski, et al., "Virtual flux based Direct Power Control of three-phase PWM rectifier", *IEEE Trans. Ind. Applications*, vol. 37, no. 4, pp. 1019-1027, Jul/Aug 2001

[8] M. Malinowski, M. Jasiński, and M. P. Kazmierkowski, "Simple Direct Power Control of three-Phase PWM Rectifier Using Space-Vector Modulation (DPC-SVM)," *IEEE Trans. Ind. Electronics",* vol. 51, no. 2, pp. 447– 454, April 2004.

[9] P. Rioual et al.," Regulation of A PWM Rectifier in The Unbalanced Network State", *Power Electron. Spec. Conf. –PESC*, Seattle, USA, 1993, pp .641-647

[10] H.S. Kim et al., "Design of Current Controller for Three-Phase PWM Converter with Unbalanced Input Voltage," *IEEE 29th Annual Power Electron. Spec. Conf. –PESC'98*, Fukuoka, Japan, 1993, pp. 503-509

[11] G. Saccomando, J. Svensson, "Transient operation of grid-connected voltage source converter under unbalanced voltage conditions," *36th IAS Annual Meeting*, vol.4, Sept. 30, 2001, pp.2419-2424

[12] A.V. Stankovic, Ke Chen, "A New Control Method for Input–Output Harmonic Elimination of the PWM Boost-Type Rectifier Under Extreme Unbalanced Operating Conditions," *IEEE Trans. Ind. Electron.",* vol.56, no.7, pp.2420-2430, July 2009

[13] D. Roiu, et al., "New Stationary Frame Control Scheme for Three-Phase PWM Rectifiers Under Unbalanced Voltage Dips Conditions," *IEEE Trans. Ind. Appl.*, vol.46, no.1, pp. 268-277, Jan.-Feb. 2010

[14] Zixin Li; et al., "Control of Three-Phase Boost-Type PWM Rectifier in Stationary Frame Under Unbalanced Input Voltage", *IEEE Transactions on Power Electronics*, vol.25, no.10, pp. 2521-2530, Oct. 2010,

[15] H.-G. Jeong, U.-M. Choi, and K.-B. Lee, "Control strategies for wind power systems to meet grid code requirements", *Proc. IEEE 37th Annu. Conf. Ind. Electron. Soc.*, 2011, pp. 1250–1255.

[16] A. Milicua, G. Abad, M.A. Rodriguez Vidal, "Online Reference Limitation Method of Shunt-Connected Converters to the Grid to Avoid Exceeding Voltage and Current Limits Under Unbalanced Operation—Part I: Theory," *IEEE Trans. Energy Conv.*, vol.30, no.3, pp.852-863, Sept. 2015

[17] Z. Ivanovic, et al., "Control of multilevel converter driving variable speed wind turbine in case of grid disturbances", *Proc. 12th Int. Power Electron. Motion Control Conf.*, 2006, pp. 1569–1573.

[18] J. A. Suul, "Control of grid integrated voltage source converters under unbalanced conditions" Ph.D. disseration, Dept. Elect. Power Eng., Norwegian Univ. Sci. Technol., Trondheim, Norway, 2012.

[19] M. Castilla, et al., "Voltage support control strategies for static synchronous compensators under unbalanced voltage sags," *IEEE Trans. Ind. Electron.*, vol. 61, no. 2, pp. 808–820, Feb. 2014.

[20] P. Rodriguez, et al., "Safe current injection strategies for a STATCOM under asymmetrical grid faults," *Proc. IEEE Energy Convers. Congr. Expo.*, 2010, pp. 3929– 3935.

[21] L. A.Serpa, et al., "A Modified Direct Power Control Strategy Allowing the Connection of Three-Phase Inverters to the Grid through LCL Filters", *IEEE Trans. Ind. Appl.*, vol.43, no.5, p. 1388-1400, Sept/Oct. 2007

[22] M. Hamouda, H. F. Blanchette, and K. Al-Haddad, "Unity Power Factor Operation of Indirect Matrix Converter Tied to Unbalanced Grid" *IEEE Trans. Power Electron.*, vol. 31, no. 2, pp. 1095-1107, Feb. 2016

[23] L. Hang and M. Zhang, "Constant power control-based strategy for Vienna-type rectifiers to expand operating area under severe unbalanced grid", *IET Power Electronics*, vol. 7, no. 1, pp. 41-49, January 2014.

[24] Y. Zhang and C. Qu, "Table-Based Direct Power Control for Three-Phase AC/DC Converters Under Unbalanced Grid Voltages", *IEEE Trans. Power Electron.*, vol. 30, no. 12, pp. 7090-7099, Dec. 2015.

[25] Y. Zhang and C. Qu, "Direct Power Control of a Pulse Width Modulation Rectifier Using Space Vector Modulation Under Unbalanced Grid Voltages," *IEEE Trans. Power Electron.*, vol. 30, no. 10, pp. 5892-5901, Oct. 2015.

[26] M. Guan and Z. Xu, "Modeling and Control of a Modular Multilevel Converter-Based HVDC System Under Unbalanced Grid Conditions," *IEEE Transactions on Power Electronics*, vol. 27, no. 12, pp. 4858-4867, Dec. 2012.

[27] H. Nian, et al, "Flexible Grid Connection Technique of Voltage-Source Inverter Under Unbalanced Grid Conditions Based on Direct Power Control," *IEEE Trans. Ind. Appl.*, vol. 51, no. 5, pp. 4041-4050, Sept.-Oct. 2015.

[28] C. Ng, L. Ran and J. Bumby, "Unbalanced Grid Fault Ride-Through Control for a Wind Turbine Inverter," *Industry Applications Conference, 2007. 42nd IAS Annual Meeting*, New Orleans, USA, 2007, pp. 154-164.

[29] F. Wang, J. L. Duarte and M. A. M. Hendrix, "Pliant Active and Reactive Power Control for Grid-Interactive Converters Under Unbalanced Voltage Dips," *IEEE Transactions on Power Electronics*, vol. 26, no. 5, pp. 1511-1521, May 2011.

[30] A. Junyent-Ferre, et al., "Current Control Reference Calculation Issues for the Operation of Renewable Source Grid Interface VSCs Under Unbalanced Voltage Sags", *IEEE Transactions on Power Electronics*, vol. 26, no. 12, pp. 3744-3753, Dec. 2011.

[31] M. Reyes, et al., "Enhanced Decoupled Double Synchronous Reference Frame Current Controller for Unbalanced Grid-Voltage Conditions," *IEEE Transactions on Power Electronics*, vol. 27, no. 9, pp. 3934-3943, Sept. 2012.

[32] G. Iwanski, et al., "Indirect Torque and Stator Reactive Power Control of Doubly Fed Induction Machine Connected to Unbalanced Power Network," in *IEEE Trans. Energy Conv.*, vol. 31, no. 3, pp. 1202-1211, Sept. 2016.

**Grzegorz Iwanski** received the M.Sc. degree in automation and robotics, and the Ph.D. degree in electrical engineering from Warsaw University of Technology (WUT), Warszawa, Poland, in 2003 and 2005, respectively. Since January 2006 to December 2008 he was a research worker in the Institute of Control and Industrial Electronics of WUT involved in international project within 6th Framework Programme of EU. Since 2009 he has been an Assistant Professor in Institute of Control and Industrial Electronics WUT. He teaches courses on power electronics, drives and power conversion systems. His research interests include variable and adjustable speed power generation systems, photovoltaic and energy storage systems, automotive power electronics and drives. In 2012/2013 he joined the team of REES UPC, Barcelona –Terrassa, within the framework of scholarship of Polish Minister of Science and Higher Education for investigation of power converters topologies with reduced common-mode component for photovoltaic systems. He is co-author of one monograph, three books chapters and about 50 journal and conference papers.

**Tomasz Łuszczyk** received MSc degree in electrical engineering from the Warsaw University of Technology (WUT) in 2011. In 2011 he started PhD course in Electrical Engineering at WUT. His research is concentrated on vector control of electic machines.

**Mateusz Szypulski** received the M.Sc. degree in automation and robotics from the Warsaw University of Technology (WUT), Warszawa, Poland, in 2012. In 2012, he started the Ph.D. course in electrical engineering at the WUT. His research interests include speed and position observers for electrical machines and applications of state feedback controllers.